Source analysis of the 2002 Molise, southern Italy, twin earthquakes (10/31 and 11/01)

Martin Vallée[1,2] and Francesca Di Luccio[3]

Received 10 February 2005; revised 4 May 2005; accepted 18 May 2005; published 24 June 2005.

[1] On October 31, 2002, a moderate size earthquake (Mw = 5.8) occurred in Molise region, southern Italy, causing loss of young human lives in a school collapse and destructions in several villages. The day after, a slightly smaller earthquake happened a few kilometers westward from the first one, without making strong damage. We use a complete set of seismological data (global, regional and local, including both body and surface waves) to better understand the source process of these two events. We show that the two earthquakes are similar, in terms of hypocentral depth, focal mechanism, and source kinematics. Moreover, the imaged slip zones are almost contiguous which makes the time delay between the two shocks (29 hours) an open question. The identified updip rupture propagation has amplified the radiation usually created by such Mw = 5.8 earthquakes at 15–20 km depth. We model a maximum acceleration zone in agreement with location of damaged villages. **Citation:** Vallée, M., and F. Di Luccio (2005), Source analysis of the 2002 Molise, southern Italy, twin earthquakes (10/31 and 11/01), *Geophys. Res. Lett.*, *32*, L12309, doi:10.1029/2005GL022687.

1. Introduction

[2] The Appenninic seismicity, central and southern Italy, is often constituted of multishock sequences, with at least two main earthquakes of similar magnitude. With a time interval between events varying between a few tenths of seconds to several months, such a behaviour was observed for Irpinia (11/23/1980), Abruzzo (1984), Potenza (Basilicata, 1990–1991) and Umbria-Marche (1997) earthquakes. In a similar way, the 2002 Molise sequence was characterized by compound earthquakes (10/31/2002 and 01/11/2002).

[3] The first shock (thereafter called MS1) occurred in the vicinity of the village of San Giuliano di Puglia (Figure 1c), where it caused the death of 29 people, most of them in the collapse of a primary school. The earthquake hypocenter was located at mid-crust depth and its mechanism was almost pure strike slip (Figure 1). The analysis of aftershock activity [*De Gori and Molise Working Group*, 2004] shows that the causal fault was the East-West striking one. The second shock (thereafter called MS2) occurred 8 km west of the first one, with very similar properties. This earthquake was strongly felt but did not cause any additional casualties. Details on the tectonic setting of this sequence are given by *Valensise et al.* [2004] and *Di Bucci and Mazzoli* [2003]. We show here how the conjoint use of various seismic data gives us information on the earthquakes source processes and how these processes are related to the damages in the epicentral area.

2. Coseismic Data

[4] We make use of a broad range of seismic data, taking into account simultaneously teleseimic, regional and local seismic signals (Figure 1). Teleseismic data come from the Global Seismic Network (GSN) and Geoscope broad-band sensors. We have selected 10 recordings for P waves and 8 for SH waves, at epicentral distances ranging between 35° and 80° (Figure 1a). The P-wave and SH-wave data of both shocks, for representative stations, can be seen in Figures 2a and 2b, respectively. The azimuthal coverage is good in the whole eastern direction, but because of the relatively small magnitudes of the events (Mw 5.7–5.8) and the large distances from North America, no good data was available at west of the earthquakes.

[5] Teleseismic data offer a good resolution about global rupture process and source depth (due to reflected phases) but they do not provide a good estimate of the earthquake lateral extension, as waves do. So we add regional data in Europe provided by Geofon and GSN networks. To avoid the difficult high frequency modelling at these distances, we use the Empirical Green Function (EGF) approach. This technique, widely used since the first studies of *Hartzell* [1978], uses the signal of a smaller event to model the Green function of the main earthquake. The usual requests for the smaller event is to be at least one degree in magnitude smaller than the mainshock and to have a similar location and focal mechanism. The study of *Di Luccio et al.* [2005], which has defined the centroid moment tensors for the main events of the Molise sequence [see *Di Luccio et al.*, 2005, Table 1] informs us of the potential candidates for an EGF. Among them, we select the 2002/11/01 17:21 earthquake (Mw = 4.5), which meets the best the EGF requirements. We have checked that results are similar with the 2002/11/12 aftershock (Mw = 4.6).

[6] We use the technique described by *Vallée* [2004], which stabilizes the classical deconvolution between the mainshock and the EGF in order to obtain more reliable Relative Source Time Functions (RSTFs). These RSTFs, obtained at various azimuths, give information on the source process itself. We apply this technique to surface waves to better detect lateral rupture directivity effects. Selected stations (see *Vallée* [2004] for the criteria of selection) are presented in Figure 1b and obtained RSTFs, for both events, can be seen in Figure 2c.

[1]Osservatorio Vesuviano, Istituto Nazionale di Geofisica e Vulcanologia, Naples, Italy.
[2]Now at Géosciences Azur, Institut de Recherche pour le Développement, Nice, France.
[3]Istituto Nazionale di Geofisica e Vulcanologia, Rome, Italy.

0094-8276/05/2005GL022687$05.00

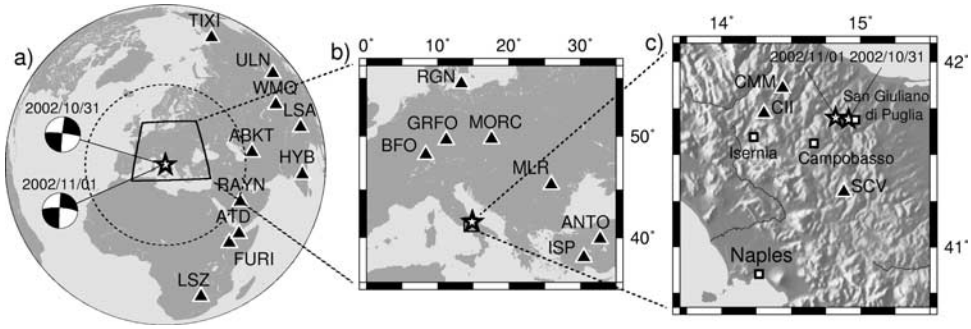

Figure 1. Receivers and earthquakes location. (a) Teleseismic stations providing P and SH recordings. All 10 stations are used for P waves whereas we have not used the SH signals of ULN and FURI, too close from the nodal planes. (b) Location of regional stations used in the EGF analysis. (c) Location of the local stations and of San Giuliano di Puglia, the most damaged village.

[7] Finally, we use local data which are even more sensitive to source size because Green functions spatially vary along the fault. No digital recordings closer than 36 km from the sources were available. Three stations, CII (MedNet broadband station), CMM and SCV (RAN, Rete Accelerometrica Nazionale, accelerometers), are at distances between 36 km and 50 km (Figure 1c). We select only the transverse component (Figure 2d) because its modelling is less dependent on accurate 3D velocity structure.

3. Source Identification Procedure

[8] The analysis of teleseismic and especially local seismic waves requires the knowledge of the source structure. To define the crustal velocity model, we use the work of *Mostardini and Merlini* [1986] to define the first kilometers, and the wide angle seismic profiles analysed by *Scarascia et al.* [1994] to define the lower crust structure. The model, presented in Table 1, remains too simple to fully explain the complexity of local data and we include in the inversion only the larger amplitude CII and SCV stations.

[9] The seismic wave field at teleseismic distances (P and SH waves) is computed using a source embedded in a layered medium [*Bouchon*, 1976; *Müller*, 1985] convolved with the mantle propagation effects (attenuation and geometrical spreading). To correct for errors in theoretical arrival times, we have manually picked the first P wave arrival. Moreover, we allow a time shift up to ±3 s for P waves and ±5 s for SH waves and select the shift corresponding to the best correlation. The local seismic wave field is calculated with the discrete wave number method [*Bouchon*, 1981] associated to the reflectivity method.

[10] The parametrisation of the source itself is done with the slip patch approach [*Vallée and Bouchon*, 2004], which describes the main earthquake characteristics in a synthetic manner: namely, we look directly for the location and size of the main slip patches on the fault. This presents the main advantage - with respect to a more classical gridded fault parameterization - to considerably reduce the number of parameters describing the faulting process. In the one-patch model case, this technique needs the definition of 10 parameters: focal mechanism (3), hypocentral depth, position of the patch with respect to the hypocenter (2), size of the elliptical patch (2), slip and rupture velocity inside the patch. Local slip duration is generally poorly resolved and we have fixed it to 0.5 s. With slip values of a few tenths of cm, it yields a slip velocity of the order of 1 m/s, in agreement with earthquake dynamics. Equations relating the body wave displacements and RSTFs to the patch(es) parameters are described by *Vallée and Bouchon* [2004]. In

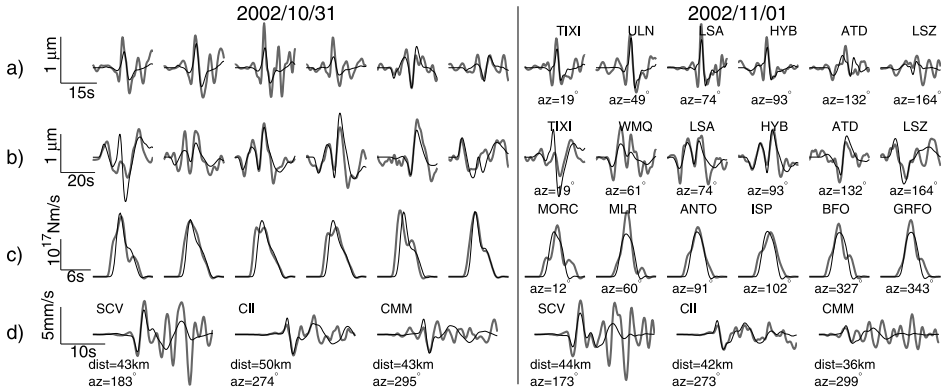

Figure 2. Agreement between data and synthetics (both lowpass filtered at 0.5 Hz) for representative stations. Waveforms relative to the MS1 are on the left and these of MS2 on the right. (a) P waves. (b) SH waves. (c) RSTFs deduced from the EGF analysis. (d) Local data; CMM station is presented but was not used to define the inverse model. Data are represented by thick gray lines whereas synthetics corresponding to the source models of Figure 3 are thin black lines. Selected stations and scales are the same for both shocks. Names and azimuths of stations are written on the right for the MS2 but, for clarity, have not been repeated for MS1. Agreement between data and synthetics at all stations can be seen in Figure A1.

Table 1. Crustal Model Used in the Source Analysis[a]

Th, km	V_P, km/s	V_S, km/s	ρ, kg/m^3	Q_P	Q_S
3.	4.	2.3	2400	300	150
28.	6.3	3.64	2750	600	300
0	8.	4.62	3250	1000	500

[a]*Th*, V_P, V_S, ρ, Q_P, Q_S are respectively the layer thickness, P-wave velocity, S-wave velocity, density and quality factor for P and S waves.

a similar manner as for body waves, we can relate the local wave field (computed in terms of discrete wave number method) to the patch parameters.

4. Source Inversion of MS1 and MS2

[11] The precise fault mechanism and hypocentral depth are crucial parameters for the source analysis and we choose to evaluate them separately. Using slip patch method only with teleseismic body waves, we determine that an hypocentral depth of 16 km for MS1 and 18 km for MS2, and a focal mechanism of (strike = 276°, dip = 84°, rake = 183°) for MS1 and (strike = 273°, dip = 76°, rake = 182°) for MS2 give the best agreement between synthetics and data. The necessity of a slightly different mechanism for both shocks can be seen for example with the noticeably different SH signals at station ATD (Figure 2b). The North-dipping plane defined for MS2 is also consistent with aftershock activity [*De Gori and Molise Working Group*, 2004].

[12] Knowing the focal depth and mechanism, we then investigate the other source characteristics by inverting simultaneously the three types of data. Given the simplicity of P, SH, and RSTFs waveforms, the introduction of a multi-patch model is not required. Thus, we aim at retrieving for both shocks the remaining 6 parameters of the one-patch model: position of the patch with respect to the hypocenter, size of the patch, slip and rupture velocity inside the patch. To do so, we minimize, in terms of L1 norm, the difference between data and synthetics (both low-pass filtered at 0.5 Hz), using the Neighborhood Algorithm (NA) [*Sambridge*, 1999]. The weight to different data is assigned in a way that one P waveform, one SH waveform, one RSTF and one local waveform have a similar importance in the inversion process. Tests done with a stronger weight for body waves logically result in a less well defined rupture lateral extension. In the misfit function, we also add the minimization of maximum slip as a slight constraint, to prevent from unphysical high stress drop models. By a repeated use of NA with different starting points, we define the mean values and standard errors of the main source parameters (Table 2). Agreement to seismic data is presented in Figure 2 and Figure A1[1]. Visualization of the best slip models is shown in Figure 3.

[13] The inversion results clearly show (Table 2 and Figure 3) that the two earthquakes are similar, not only in terms of depth, magnitude and focal mechanism, but also in terms of source kinematics. In particular both earthquakes exhibit a clear updip rupture propagation, with the rupture reaching about 6 km deep for MS1 and 9 km for MS2. MS1 is found only a bit larger (Mw = 5.8 versus Mw = 5.7), with a longer duration (5.4 s versus 4.1 s). The resolution on lateral extent is lower for MS1 because of a stronger trade-off with average slip in the patch (thus giving similar global moment). Rupture velocity as low as 1.1 km/s for MS1 was already identified in the preliminary source model of *Di Luccio et al.* [2005]. Using a larger number of seismic stations and different types of data, we confirm here a rather low rupture velocity (2 km/s, representing 55% of the shear velocity), but closer to classical models of earthquake rupture.

Table 2. Source Parameters Defined by the One-Patch Model Inversion for the 10/31/2002 (MS1, Hypocentral Depth = 16 km) and 01/11/2002 (MS2, Hypocentral Depth = 18 km) Shocks[a]

	MS1	MS2
Moment (10^{17} N.m)	5.46 (±0.16)	3.58 (±0.1)
Duration, s	5.39 (±0.13)	4.1 (±0.11)
Average slip, m	0.25 (±0.14)	0.15 (±0.02)
Rupture velocity, km/s	2.01 (±0.23)	2.56 (±0.19)
Top depth, km	6.03 (±1.08)	9.02 (±0.59)
Bottom depth, km	20.15 (±0.67)	18.43 (±0.12)
Eastward extension, km	2.46 (±0.57)	3.82 (±0.3)
Westward extension, km	2.74 (±1.28)	4.75 (±0.49)

[a]We present mean values and standard errors (between brackets) deduced from the 10 best models coming from 10 independent runs of NA.

[14] Our inversion for MS1 can also be compared with the work of *Gorini et al.* [2004]. Modelling peak ground accelerations, this study has identified both an updip and eastern rupture propagation. This latter property is not retrieved with our data, because the small variation of the RSTFs with azimuth constitutes a strong evidence for a bilateral rupture propagation. We also note that the eastern directivity is not obvious in the distribution of seismic intensities (http://www.ingv.it/roma/reti/rms/terremoti/italia/molise/molise.html).

5. Discussion

[15] We have shown that the two main earthquakes of the Molise sequence are kinematically similar, and that their

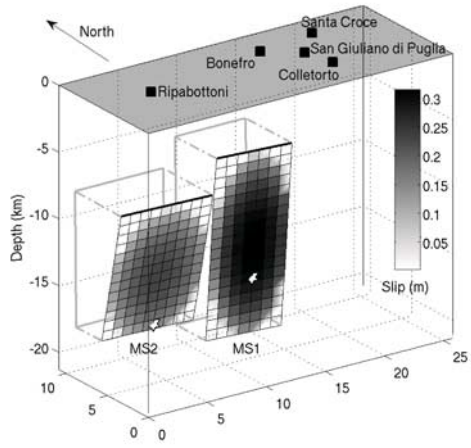

Figure 3. 3D visualization of the earthquakes slip showing that the two imaged slip patterns are almost contiguous. We present here typical slip models, which are the best models given by NA the closest from the mean values of Table 2. Hypocenters are indicated by white stars and map scales (East, North, vertical) are in km.

[1]Auxiliary material is available at ftp://ftp.agu.org/apend/gl/2005GL022687.

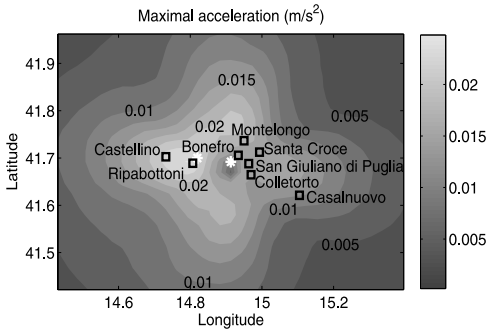

Figure 4. Location of maximum acceleration areas compared to the location of villages having experienced a seismic intensity superior or equal to VII.

slip patterns are almost contiguous. Postseismic activity [*Castello et al.*, 2005] is interestingly related with slip distribution. Few aftershocks occurred at depths between 10 and 20 km - where coseismic slip was large - whereas deeper and especially shallower events were much more common. In terms of earthquake mechanics, the main question that rises from this study is the 29 hour delay between the two events. Considering the spatial vicinity between the two shocks, it is interesting that the second event has not been dynamically triggered by the first one, resulting in a Mw = 6.0 earthquake. It shows that the distances between the two faults (of the order of 1 km) and/or their dip difference (8°) were enough to play the role of a barrier. As discussed by *Di Luccio et al.* [2005], low seismic energy, consistent with slow rupture velocity, could explain why the first shock was unable to dynamically trigger the second one. This example is as puzzling as the 1997 Umbria-Marche sequence, where two closely related earthquakes were separated by a 9 hour-delay [*Hernandez et al.*, 2004].

[16] Concerning seismic damage, the updip rupture propagation has had two important consequences. The more obvious one is the presence of slip close to the Earth surface (up to 6 km deep for MS1). The other one is the occurrence of the well-known directivity effect, which amplifies the radiation in the direction of the rupture propagation. The stronger damages due to MS1 in comparison to MS2 can be attributed to the combination of the following factors: (1) slightly larger seismic moment, (2) shallower top depth of the rupture and (3) epicenter closer to San Giuliano di Puglia in which site effects are particularly strong [*Azzara et al.*, 2003]. In terms of seismic risk assessment, this mid-crustal seismicity should be carefully considered in particular if the updip propagation generally characterizes the rupture process. Analysis of 2002 Molise aftershocks (Mw = 4–4.5), for which a denser accelerometric array was present, should be able to answer this question.

[17] In conclusion, we model in Figure 4 the location of maximum accelerations generated by the destructive first shock (MS1). To do so, we use our kinematical model (Figure 3) and calculate the seismic radiation on each point of a 2.5 × 2.5 km^2 grid (global size equal to 80 × 60 km^2) with the discrete wave number method [*Bouchon*, 1981]. This approach, purely deterministic, is not a strong motion simulation in which contributions from 3D structure, high frequency radiation and site effects should be included. In this sense we do not aim at retrieving realistic values of seismic accelerations. But finite-extent source effects (source extension, directivity) are present in the calculation and so, this method is able to provide an estimate, quickly and simply after an earthquake, of the potentially damaged zone. Figure 4 represents the maximum acceleration values (below 0.5 Hz) in the epicentral area. The East-West elongation of the maximum radiation area is in agreement with the villages having experienced a seismic intensity equal or superior to VII.

[18] **Acknowledgments.** We thank P. De Gori, A. Herrero, L. Improta, A. Zollo, G. Iannaccone, and N.A. Pino for fruitful discussions. This study has also been improved by the careful reviews of J. Zahradnik and Y. Yagi. We are grateful to GSN, GEOFON, Geoscope, and MedNet networks for access to broadband data and to the RAN (Rete Accelerometrica Nazionale, managed by the Servizio Sismico Nazionale) for access to accelerometric data. GMT and Latex free softwares were helpful to the preparation of the manuscript. This work was funded by the European "Marie Curie" fellowship MEIF-CT-2003-500901.

References

Azzara, R. M., T. Braun, F. Cara, G. Cultrera, G. Di Giulio, F. Marra, and A. Rovelli (2003), The ML 5.4 Molise earthquake (central Italy) of October 31, 2002: Why so destructive effects in San Giuliano di Puglia, *Geophys. Res. Abstr.*, *5*, 09611.

Bouchon, M. (1976), Teleseismic body wave radiation from a seismic source in a layered medium, *Geophys. J. R. Astron. Soc.*, *47*, 515–530.

Bouchon, M. (1981), A simple method to calculate Green's functions for elastic layered media, *Bull. Seismol. Soc. Am.*, *71*, 959–971.

Castello, B., G. Selvaggi, C. Chiarabba, and A. Amato (2005), *CSI Catalogo Della Sismicita Italiana 1981–2002, Versione 1.0*, Ist. Naz. di Geofis. e Vulcanol., Rome. (Available at http://www.ingv.it/CSI.)

De Gori, P., and Molise Working Group (2004), A first analysis of the 2002 Molise earthquake seismic sequence, *Geophys. Res. Abstr.*, *6*, 04040.

Di Bucci, D., and S. Mazzoli (2003), The October–November 2002 Molise seismic sequence (southern Italy): An expression of Adria intraplate deformation, *J. Geol. Soc. London*, *160*, 503–506.

Di Luccio, F., E. Fukuyama, and N. A. Pino (2005), The 2002 Molise earthquake sequence: What can we learn about the tectonics of southern Italy?, *Tectonophysics*, in press.

Gorini, A., S. Marcucci, P. Marsan, and G. Milana (2004), Strong motion records of the 2002 Molise, Italy, earthquake sequence and stochastic simulation of the main shock, *Earthquake Spectra*, *20*, S65.

Hartzell, S. H. (1978), Earthquake aftershocks as Green's functions, *Geophys. Res. Lett.*, *5*, 1–4.

Hernandez, B., M. Cocco, F. Cotton, S. Stramondo, O. Scotti, F. Courboulex, and M. Campillo (2004), Rupture history of the 1997 Umbria-Marche (central Italy) main shocks from the inversion of GPS, DInSAR and near field strong motion data, *Ann. Geophys.*, *47*, 1355–1376.

Mostardini, F., and S. Merlini (1986), Appennino centro-meridionale: Sezioni geologiche e proposta di modello strutturale, *Mem. Soc. Geol. It.*, *35*, 177–202.

Müller, G. (1985), The reflectivity method: A tutorial, *J. Geophys.*, *58*, 153–174.

Sambridge, M. (1999), Geophysical inversion with a neighbourhood algorithm. I. Searching a parameter space, *Geophys. J. Int.*, *138*, 479–494.

Scarascia, S., A. Lozej, and R. Cassinis (1994), Crustal structures of the Ligurian, Tyrrhenian and Ionian seas and adjacent onshore areas interpreted form wide angle seismic profiles, *Boll. Geofis. Teor. Appl.*, *36*, 5–19.

Valensise, G., D. Pantosti, and R. Basili (2004), Seismology and tectonic setting of the Molise, Italy, earthquake, *Earthquake Spectra*, *20*, S23.

Vallée, M. (2004), Stabilizing the empirical Green function analysis: Development of the projected Landweber method, *Bull. Seismol. Soc. Am.*, *94*, 394–409.

Vallée, M., and M. Bouchon (2004), Imaging coseismic rupture in far field by slip patches, *Geophys. J. Int.*, *156*, 615–630.

F. Di Luccio, Istituto Nazionale di Geofisica e Vulcanologia, I-00143 Rome, Italy.

M. Vallée, Géosciences Azur, IRD, F-06560 Valbonne, France. (vallee@geoazur.unice.fr)